Acknowledgment. This work was supported by The Robert A. Welch Foundation Grant No. A-259 (A.E.M. and E.C.N.) and National Science Foundation Grant No. CHE79-16160 (A.C. and P.R.).

Registry No. *cis*-$[Co(C_{10}H_8N)_2CO_3]NO_3 \cdot 5H_2O$, 82583-18-4; *cis*-$[Co(C_{12}H_8N_2)_2CO_3]Br \cdot 4H_2O$, 74325-78-3.

Supplementary Material Available: Calculated and observed structure factors for complex **4** (Table A) and complex **5** (Table B), hydrogen atom positional and thermal parameters (Table C), complete bond distances and bond angles for **4** (Table D) and **5** (Table E), least-squares planes for **4** (Table F) and **5** (Table G), and representative infrared spectra for **4** and **5** (Figure A) (21 pages). Ordering information is given on any current masthead page.

Contribution from the Istituto di Chimica Generale ed Inorganica, Università di Padova, 35100 Padova, Italy, Istituto di Chimica Generale ed Inorganica, Università di Parma, 43100 Parma, Italy, Institut de Chimie, Université Louis Pasteur, Strasbourg, France, and Institut für Anorganische Chemie, Universität Regensburg, D-8400 Regensburg 1, West Germany

Molecular Structure and Experimental Electron Density of (μ-Methylene)bis[dicarbonyl(η^5-cyclopentadienyl)manganese] at 130 K[1]

DORE A. CLEMENTE,*[2,3] M. CINGI BIAGINI,[4] BERNARD REES,[2] and WOLFGANG A. HERRMANN[5]

Received November 30, 1981

The molecular structure and the experimental electron-density distribution of $(\mu\text{-}CH_2)[CpMn(CO)_2]_2$ at 130 K have been determined from single-crystal X-ray diffraction data up to $(\sin\theta)/\lambda = 1.06$ Å^{-1} with use of the X–X technique. The electron deformation density maps revealed no significant charge density accumulation on the Mn–Mn bond, in contrast with the other bonds: 0.55 e Å^{-3} in the C–C bonds of the cyclopentadienyl group, 0.90 e Å^{-3} in C–O. Peaks are also observed in the carbon lone-pair region of the CO groups (0.70 e Å^{-3}) and in the metal region: the latter are essentially concentrated along the axis joining Mn to the centroid of the cyclopentadienyl ring and in a plane almost parallel to the cyclopentadienyl ring, at a distance of about 0.60 Å from the metal nucleus. A charge accumulation corresponding to a σ lone pair of methylene is visible. Atomic charges were determined both by least-squares refinement and by direct integration. Both methods indicate small charges. The carbonyl oxygen atoms are predicted to be negative and so are the carbon atoms of the cyclopentadienyl rings. Mn atoms seem also slightly negative; however, the diffuseness of the 4s shell makes this charge difficult to determine. While all theoretical calculations predict a large negative charge on the methylene carbon, the experimental charge is not significantly different from zero.

Introduction

A number of structural and chemical investigations have been carried out recently on μ-methylene complexes.[6] The theory of bonding in such complexes[7] shows that bridging methylene can act as a σ donor to the metal through a filled a_1 orbital and as a π-electron acceptor using a high-lying p_π empty orbital of symmetry b_1. In this respect bridging methylene thus shows some analogy with bridging carbonyl. On the other hand theoretical studies[8] have shown that the methylene carbon is negatively charged. No experimental determination of the charge density distribution in this class of compounds has been done as yet, and it seemed therefore interesting to submit the title compound to a so-called X–X analysis.

Also of interest is the metal–metal bond, formally of multiplicity 1. The title compound is analogous with $Mn_2(CO)_{10}$ but with a Mn–Mn separation about 0.1 Å shorter. In $Mn_2(CO)_{10}$, as in most metal–metal-bonded complexes studied so far, no significant charge density accumulation had been observed in the middle of the bond.[9]

The purpose of the present study is to determine accurately the molecular structure, the electron-density distribution, and the atomic charges in order to gain a better understanding of the bonding in this class of μ-methylene compounds. A preliminary account of part of this work has been given elsewhere.[10]

Table I. Crystal Data and Data Collection

Crystal Data
trans-$(\mu\text{-}CH_2)[(\eta^5\text{-}C_5H_5)Mn(CO)_2]_2$
cryst: space group $Pccn$ (D_{2h}^{10}, No. 56); $Z = 4$
unit cell at room temperature:[a] $a = 7.275$ (6), $b = 15.367$ (8), $c = 12.835$ (8) Å; $V = 1434.9$ Å^3
unit cell at 130 K:[a] $a = 7.161$ (4), $b = 15.177$ (6), $c = 12.703$ (6) Å; $V = 1380.6$ Å^3
cryst I: spherical; diameter 0.28 ± 0.02 mm
cryst II: spherical; diameter 0.33 ± 0.02 mm
abs: linear abs coeff $\mu = 19.24$ cm^{-1} ($\mu R_1 = 0.27$, $\mu R_2 = 0.32$)
transmission factor: cryst I, 0.671–0.681; cryst II, 0.626–0.638
weighted path length $\bar{T}$: cryst I, 0.019–0.020 cm; cryst II, 0.022–0.024 cm
Diffraction Measurements
scanning mode: continuous $\omega/2\theta$
scanning interval in θ: cryst I, 1.6 + 0.2 tan θ; cryst II, 1.7 + 0.2 tan θ
scanning speed in ω: 2.4° min^{-1}
bkgd determn: during 20 s at each end of the interval
no. of measmts up to $(\sin\theta)/\lambda$: 1.06 Å^{-1} ($\theta = 49°$) not including std reflctns: cryst I, 7430 reflctns ($\bar{h}kl$, and some $\bar{h}kl$); cryst II, 14 026 reflctns (hkl, $\bar{h}\bar{k}l$, and some $\bar{h}kl$)

[a] As the mean of two spherical samples.

Experimental Section

Air-stable crystals of $(\mu\text{-}CH_2)[CpMn(CO)_2]_2$ (Cp = C_5H_5) were obtained by recrystallization from pentane at −78 °C and were ground

(1) Research was carried out at the Università di Padova e Parma, at the Université Louis Pasteur, and at the Universität Regensburg under contract with the Italian CNR for international projects and supported by the Italian CNR by Grant Nos. 80.00317.03 and 81.00581.03.
(2) Université Louis Pasteur.
(3) Present address: Università di Padova.
(4) Università di Parma.
(5) Universität Regensburg.
(6) W. A. Herrmann, *Adv. Organomet. Chem.*, **20**, 159 (1982).
(7) D. C. Calabro, D. L. Lichtenberger, and W. A. Herrmann, *J. Am. Chem. Soc.*, **103**, 6852 (1981).
(8) P. Hofmann, *Angew. Chem., Int. Ed. Engl.*, **18**, 554 (1979).
(9) M. Martin, B. Rees, and A. Mitschler, *Acta Crystallogr., Sect. B*, **B38**, 6 (1982).
(10) D. A. Clemente, B. Rees, G. Bandoli, M. Cingi Biagini, B. Reiter, and W. A. Herrmann, *Angew. Chem., Int. Ed. Engl.*, **20**, 887 (1981).

0020-1669/82/1321-3741$01.25/0

into spheres with use of the Nonius crystal grinder. Two small, almost spherical samples were selected, and their mean radius was determined under a high-magnification microscope. Low-temperature X-ray diffraction intensities were collected on a Philips PW-1100 diffractometer with graphite-monochromated Mo Kα radiation for both samples. The stability of the instrument was monitored by measuring three standard reflections at intervals of 100 min. Variations in the intensities were on the average 3%, while the maximum variation was 3.8%. The crystals were cooled by a stream of cold nitrogen directed at them from the top (Leyboldt-Heraeus, NCD1 cooling device). By indirect measurement, using a chromel–alumel thermocouple, the temperature at the crystals was estimated to be 130 ± 4 K. The cell constants at this temperature were determined by a least-squares refinement of the setting angles of 25 reflections (Mo $K\alpha_1$ radiation, $\lambda = 0.7093$ Å; $2\theta \simeq 50°$).

The cell parameters at room temperature were determined with essentially the same technique but with 25 reflections of lower θ values and λ(Mo Kα) = 0.7107 Å radiation. Other crystallographic and data collection characteristics are given in Table I.

Data Processing and Structure Determination. The distribution of the standard reflections was analyzed by means of the program STANDARD (an unpublished program by B.R.). This program determines a time-dependent scaling factor as well as a time-dependent instability term to be added to the variance on the basis of counting statistics.[11] After the Lorentz and polarization corrections the diffracted intensities were also corrected for absorption by interpolation from calculated tables,[12] and the absorption-weighted path lengths were calculated by following the method of ref 13 (program written by R. Wiest at Strasbourg University). The scale factor between the two sets of reflections of crystals I and II was determined by a least-squares procedure in a modified version of the program SORT, which also averages the intensities of all common and crystallographically equivalent reflections and adds a term p^2I^2 to the variance $\sigma^2(I)$. The factor p, determined from the dispersion of equivalent reflections, turned out to be 0.035.

A total of 21 456 reflections were processed, and 6986 independent reflections were obtained, of which 633 had zero or negative measured intensity. Only the 4283 independent reflections with $I > 3\sigma(I)$ were used for the structure determination. Since there are only four formula units per unit cell, the molecule must be in a special position on the twofold axis. This implies that the molecule is in the trans conformation; also NMR studies have shown that in solution only the trans conformation is present.[14] A three-dimensional Patterson map showed the position of the Mn atom, with x_{Mn} very near $^1/_4$. The difference Fourier map, phased only by Mn, duplicates all maxima by a false mirror at $x = {}^1/_4$; this was ascribed to the peculiar position of the Mn atom near the c glide perpendicular to x. This introduces a pseudoperiodicity of $c/2$ for the Mn atoms, which explains why the hkl reflections with $l = 2n$ are stronger than those with $l = 2n + 1$. Among the maxima, only those representing chemically reasonable atoms were introduced and repeated Fourier syntheses were performed until the molecular model was completed. With the aid of the full-matrix least-squares program LINEX, several cycles of refinement were performed on F_o^2 with weights $w = \sigma^{-2}(F_o^2)$. X-ray spherical-atom form factors and anomalous dispersion factors used in the least-squares refinements were taken from ref 15. Isotropic thermal parameters were used, but when R reached a value lower than 0.10, anisotropic temperature factors were introduced for the non-hydrogen atoms. At this point, although the positions of the hydrogen atoms were correct (mean C–H 0.95 Å), it was noted that their isotropic temperature factors were always near zero or even negative. Replacement of the hydrogen free-atom form factor by the form factor of Stewart, Davidson, and Simpson[16] (corresponding to a more contracted hydrogen atom) resulted in realistic isotropic thermal parameters.

Table II. Data Processing and R Factors

	full set	high angle
agreement between equiv reflctns, $\Sigma\langle[I - I_m]\rangle\Sigma I_m$ = av intensity)	0.040	0.102
no. of reflctns for least-squares input (after averaging)	4283	4955
intensity requirements	$I \geq 3\sigma(I)$	none
$R(F) = \Sigma\|\|F_o\| - K\|F_c\|\|/\Sigma\|F_o\|$	0.040	0.110
$R_w(F^2) = [\Sigma w(\|F_o\|^2 - \|KF_c\|^2)^2/\Sigma w\|F_o\|^4]^{1/2}$	0.086	0.101
$S(F^2) = [\Sigma w(\|F_o\|^2 - \|KF_c\|^2)^2/(N_{obsd} - N_{var})]^{1/2}$	1.89	1.30

Table III. Relative Coordinates (×10⁵; ×10⁴ for H)

		x	y	z
Mn	a	24244 (2)	15784 (1)	16963 (1)
	b	24238 (3)	15784 (1)	16963 (1)
C(1)	a	7593 (17)	18097 (7)	27135 (9)
	b	7591 (21)	18094 (9)	27128 (10)
O(1)	a	−3604 (15)	18661 (7)	33700 (7)
	b	−3630 (23)	18650 (10)	33715 (11)
C(2)	a	4798 (18)	12810 (8)	9015 (9)
	b	4779 (21)	12813 (10)	9024 (11)
O(2)	a	−7649 (14)	10759 (7)	3813 (8)
	b	−7679 (25)	10733 (15)	3796 (14)
C(3)	a	25000	25000	5438 (12)
	b	25000	25000	5431 (13)
C(4)	a	47263 (18)	8793 (8)	9725 (11)
	b	47241 (25)	8782 (11)	9692 (15)
C(5)	a	34820 (19)	2673 (7)	14460 (12)
	b	34808 (25)	2674 (10)	14459 (16)
C(6)	a	34285 (19)	4403 (7)	25405 (11)
	b	34264 (27)	4394 (10)	25400 (16)
C(7)	a	46367 (19)	11671 (8)	27439 (11)
	b	46327 (25)	11650 (11)	27469 (14)
C(8)	a	54354 (17)	14289 (7)	17758 (11)
	b	54432 (20)	14322 (9)	17757 (16)
H(3)	a	3538 (29)	2397 (12)	116 (14)
H(4)	a	4993 (26)	927 (12)	276 (16)
H(5)	a	2784 (26)	−184 (13)	1072 (19)
H(6)	a	2651 (24)	172 (13)	3045 (16)
H(7)	a	4920 (28)	1396 (12)	3420 (14)
H(8)	a	6226 (28)	1891 (13)	1663 (14)

[a] From conventional refinement of the full set of X-ray data, with the condition $I_{obsd} > 3\sigma(I_{obsd})$. [b] From high-order refinement $(\sin\theta)/\lambda > 0.70$ Å^{-1}, with all reflections included.

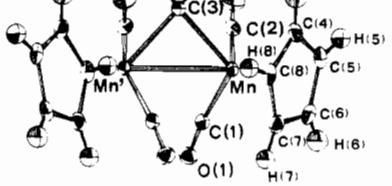

Figure 1. Molecular structure of $(\mu\text{-}CH_2)[CpMn(CO)_2]_2$ at 130 K. The numbering system used is shown. The drawings were obtained with ORTEP, and the thermal vibration ellipsoids are scaled to enclose 50% probability.

Secondary isotropic extinction, dominated by mosaic spread with a Lorentzian distribution function, was assumed, and the corresponding parameter g was refined, according to the method of Becker and Coppens.[17] Since g remained very small and of the order of its standard deviation, no extinction correction was performed in the final stages.

In the next step, a high-angle refinement was performed with use of all the 4955 reflections with $\theta > 30°$ (i.e., $(\sin\theta)/\lambda > 0.70$ Å^{-1}) with no condition on the intensity. The cyclopentadienyl hydrogen atoms were kept fixed at their geometrical position, imposing a C–H

(11) L. E. McCandlish, G. H. Stout, and L. C. Andrews, *Acta Crystallogr., Sect. A*, **A31**, 245 (1975).
(12) C. W. Dwiggins, Jr., *Acta Crystallogr., Sect. A*, **A31**, 395 (1975).
(13) H. D. Flack and G. Vincent, *Acta Crystallogr., Sect. A*, **A34**, 489 (1978).
(14) W. A. Herrmann, B. Reiter, and H. Biersack, *J. Organomet. Chem.*, **97**, 245 (1975).
(15) "International Tables for X-ray Crystallography", Vol. IV, Kynoch Press, Birmingham, England, 1974.
(16) R. F. Stewart, E. R. Davidson, and W. T. Simpson, *J. Chem. Phys.*, **42**, 3175 (1965).
(17) P. Becker and P. Coppens, *Acta Crystallogr., Sect. A*, **A31**, 417 (1975).

Table IV. Bond Lengths (Å) and Angles (Deg) in $(\mu\text{-}CH_2)[CpMn(CO)_2]_2$

Lengths

	high-order X-ray data[a]	high-order cor for thermal librations		high-order X-ray data	high-order cor for thermal librations
Mn-Mn′	2.7996 (11)	2.802	C(4)-C(5)	1.421 (3)	1.425
Mn-C(1)	1.792 (2)	1.795	C(5)-C(6)	1.415 (3)	1.419
Mn-C(2)	1.778 (2)	1.782	C(6)-C(7)	1.424 (3)	1.428
Mn-C(3)	2.026 (2)	2.028	C(7)-C(8)	1.423 (3)	1.427
Mn-C(4)	2.167 (2)	2.169	C(4)-C(8)	1.422 (3)	1.426
Mn-C(5)	2.152 (2)	2.155	C(3)-H(3)	0.93 (2)	
Mn-C(6)	2.157 (2)	2.160	C(4)-H(4)	0.91 (2)	
Mn-C(7)	2.163 (2)	2.165	C(5)-H(5)	0.97 (2)	
Mn-C(8)	2.176 (2)	2.179	C(6)-H(6)	0.94 (2)	
Mn-C_c	1.794 (2)	1.797	C(7)-H(7)	0.95 (2)	
C(1)-O(1)	1.163 (2)	1.167	C(8)-H(8)	0.91 (2)	
C(2)-O(2)	1.156 (2)	1.163			

Angles[b]

C(3)-Mn-Mn′	46.30 (4)	Mn-C(3)-Mn′	87.40 (7)
C(1)-Mn-Mn′	80.24 (5)	C(5)-C(4)-C(8)	107.80 (18)
C(2)-Mn-Mn′	106.50 (5)	C(4)-C(5)-C(6)	108.40 (15)
C(1)-Mn-C(2)	86.39 (8)	C(5)-C(6)-C(7)	107.90 (16)
C(1)-Mn-C(3)	113.82 (6)	C(6)-C(7)-C(8)	107.93 (16)
C(2)-Mn-C(3)	77.65 (6)	C(4)-C(8)-C(7)	107.97 (14)
Mn-C(1)-O(1)	172.79 (13)	H(3)-C(3)-H(3)′	108.8 (1.6)
Mn-C(2)-O(2)	178.63 (16)		

[a] Bond lengths and angles involving hydrogen atoms are obtained obviously with the coordinates of the full set. [b] From high-order X-ray data.

distance of 1.075 Å. It is not possible to know a priori the exact position of the methylene hydrogens. It was assumed that the CH directions given by the full-angle refinement were correct and that only the bond lengths needed to be adjusted. Neutron diffraction would clearly be necessary for a more precise localization.

Agreement factors and other information on data processing are given in Table II. The "goodness of fit" for the high-order data is close to 1, and this means that the spherical free-atom model is approximately correct. The positional parameters obtained from the refinement of the full and high-order data are given in Table III. Anisotropic thermal parameters U_{ij} are available (see the supplementary material).

Molecular Geometry and Dimensions

The molecule with thermal ellipsoids at the 50% probability level is shown in Figure 1. Bond lengths and angles reported in Table IV were obtained with the positional parameters derived from the refinement of the high-order data set; those of the full set are not reported because none of the bond lengths differed by more than twice the estimated standard deviation.

Results concerning three planes of chemical interest in the molecule are given in supplementary material.

The bond lengths of the cyclopentadienyl ring were corrected for thermal motion in the hypothesis that the ring behaves as a rigid body, as shown by a TLS calculation.[18] The Cp ring has a large libration motion around the axis perpendicular to its plane, with a root-mean-square amplitude of 4.0°, compared to 2.4 and 2.0° around the axes in the plane. Although the rest of the molecule is not rigid, the rigid-body approximation was used to correct the other bonds with exception of the Mn–C–O groups, for which a librational motion of the carbonyls around Mn was assumed. This motion is larger for C(2)O(2) than for C(1)O(1) (angular amplitude around Mn: C(1) = 2.67°, O(1) = 3.14°, C(2) = 3.35°, O(2) = 3.79°). This could be related with the larger value observed for the

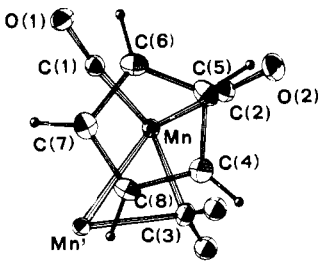

Figure 2. Projection of $(\mu\text{-}CH_2)[CpMn(CO)_2]_2$ along the C_5 axis of one cyclopentadienyl ring. For clarity only a half-molecule, together with atom Mn′, is shown.

Mn–C(1) bond length, compared to that for Mn–C(2). However the difference is only marginally reduced by the thermal libration correction (0.013 Å after correction, 0.014 Å before; see Table IV). Theoretical calculations using an idealized model (see below) do not explain such a difference. It is very unlikely that another model for thermal motion corrections would suppress the difference. More probably, the bending of Mn–C(1)–O(1) to 172.85° reduces the overlap between the 5σ carbonyl orbital and the d orbital of Mn, thus reducing the strength of the Mn–CO bond. The deviation from linearity of Mn–C(1)–O(1) (Table IV) can be ascribed to the short (2.57-Å) intramolecular contact O(1)···H(7)′ (hereafter a prime denotes the operation of the binary axis) at a right angle to CO (C(1)–O(1)···H(7)′ = 90.4°).

It is convenient to describe the molecule as two $CpMnR_3$ entities sharing a common carbon atom, each entity closely recalling the $CpMn(CO)_3$ molecule. Figure 2 shows half a molecule along an axis perpendicular to the Cp ring.

The major distortion comes from the position of the methylene carbon atom C(3), which is shifted toward the carbonyl atom C(2) (C(3)–C(2) = 2.392 Å, C(3)–C(1) = 3.201 Å; see Figure 2). The angles C_c–Mn–C(1), C_c–Mn–C(2), and C_c–Mn–C(3) (C_c denotes the centroid of the cyclopentadienyl ring) are approximately equal (122.03 (8), 121.38 (8), and 120.98 (7)°, respectively) and very close to that of $CpMn(CO)_3$, mean 123.73°,[19] or to 123°, the value suggested by Elian and Hoffmann on quantum-chemical grounds for the d^6 $Mn(CO)_3^+$ fragment.[20]

The distances from Mn to the C atoms of the Cp ring (mean 2.163 Å), are similar to those observed in $CpMn(CO)_3$ (mean 2.15 Å), suggesting analogous bonding mechanisms between Cp and the MnR_3 moiety. In $CpMn(CO)_3$ it has been described as a donation of the six electrons of the Cp^- group to the set of the three acceptor molecular orbitals of $a_1 + e$ symmetry that are constituted principally by the (xz, yz) and z^2 metal d orbitals.

In most π-bonded cyclopentadienyl complexes there is some variation in the carbon–carbon bond lengths of the Cp ligand. A good example is the compound $[CpFe(CO)_2]_2$,[21] where this feature was attributed to orbital population predominance of the antisymmetric (relative to the mirror plane of the Cp ring) e_1^+ orbital with respect to the symmetric e_1^- orbital (1.77 against 1.64). In our compound all the C–C bond lengths are equal, in agreement with the SCCC MO calculation (see below), which gives orbital populations of 1.64 and 1.60 for e_1^+ and e_1^-, respectively.

Hofmann[8] has indicated that the H–C–H angle in methylene-bridged complexes depends upon the repulsive 4-electron interaction between the $\pi(CH_2)$ orbital and the metal–metal bonding π_{xz} orbital (with x taken along the metal–metal axis

(18) V. Schomaker and K. N. Trueblood, *Acta Crystallogr., Sect. B*, **B24**, 63 (1968).

(19) A. F. Berndt and R. E. Marsh, *Acta Crystallogr.*, **16**, 118 (1963).
(20) See Table III, p 1069, in M. Elian and R. Hoffmann, *Inorg. Chem.*, **14**, 1058 (1975).
(21) A. Mitschler, B. Rees, and M. S. Lehmann, *J. Am. Chem. Soc.*, **100**, 3390 (1978).

and z normal to the M–C–M plane). Since in the Mn case the π_{xz} orbital is further away in energy than in $(\mu\text{-}CH_2)[CpRh(CO)]_2$, where an angle of 110.4 (1)° was found by neutron diffraction,[22] the H–C–H angle should be smaller in the Mn complex. Hofmann predicted an optimized value of about 100°, while from the present work the experimental angle is near the tetrahedral value: 108.8 (1.6)°.

The manganese–methylene carbon bond length 2.025 (1) Å shows that this bond has a partial double-bond character, the predicted single-bond distance for the Mn–C bond being 2.24 Å.[23]

In a summary of the molecular geometry of compounds with $M\text{–}(\mu\text{-}CH_2)\text{–}M$ cores recently reported[6,22] it may be noted that the M–C(bridging) distance is always shorter than the single-bond distance. The bonding features of bridging methylene were discussed by many authors.[6,8] The CH_2 group has a filled a_1 orbital that is used as a σ donor while it possesses also a high-lying b_1 p_π empty orbital acting as a π acceptor of electron density from the metals. Moreover the carbene ligand is oriented approximately perpendicular to M···M (the angle between the methylene plane and the dimetallacyclopropane ring Mn, C(3), Mn′ is 80.35°; see the supplementary material), so that there is an optimum overlap between the unfilled p_π CH_2 orbital and the metal–metal occupied antibonding π^*_{xy} orbital.[8] The important result is an electron transfer from the metals to the carbon atom, which thus becomes negatively charged. This charge distribution will be discussed next.

Determination of Atomic Charges

Atomic charges were determined both in reciprocal space by least-squares refinement and in real space by direct integration. In the first case a refinement of the population and radial dependence of the spherical atomic valence shell was carried out with the κ-refinement method introduced by Coppens et al.[24] This was done with the program LINEXV, a modification of the local version of the conventional least-squares refinement program LINEX. LINEXV allows the simultaneous refinement of structure, charge, and extinction parameters (the total charge of the molecule is constrained to remain invariant by the method described by Hamilton[25]). In all refinements the two O atoms were constrained to have the same contraction coefficient κ, and so were the two carbonyl C atoms and the five C atoms and the five H atoms of the cyclopentadienyl ring. The refinements were performed on F_o^2 by minimizing the quantity $R_w(F^2)$; the 4283 reflections of the full data set with $I > 3\sigma(I)$ were used but some least-squares cycles were repeated with all the 6986 reflections. The two types of refinement gave consistent results.

The core scattering factors for C and O were defined as $C_{core} = C°(RHF) - 2\langle J_o\rangle_{2s} - 2\langle J_o\rangle_{2p}$ and $O_{core} = O°(RHF) - 2\langle J_o\rangle_{2s} - 4\langle J_o\rangle_{2p}$, where the first term is the free-atom form factor and the $\langle J_o\rangle$'s are defined and tabulated in ref 15 (Table 2.2.D). The valence shell scattering factor for one electron was consequently defined as $^1/_2\langle J_o\rangle_{2s} + {}^1/_2\langle J_o\rangle_{2p}$ for C and $^1/_3\langle J_o\rangle_{2s} + {}^2/_3\langle J_o\rangle_{2p}$ for O. The free-atom Hartree–Fock form factor was taken for hydrogen. The Mn core was given by $Mn_{core} = Mn°(RHF) - 5\langle J_o\rangle_{3d} - 2\langle J_o\rangle_{4s}$. The choice of the valence shell scattering factors of Mn is more difficult; it was first assumed to be a combination of 3d and 4s types according to $f_{Mn} = {}^5/_7\langle J_o\rangle_{3d} + {}^2/_7\langle J_o\rangle_{4s}$ as in the free atom, but a pure

Table V. Atomic Charges (in Electrons)

	κ refinement								integration in real space			thcor computation		
	Mn valence shell $3d^54s^2$				Mn valence shell $3d^7$									
	IA		IIA		IB		IIB			normalized charge[a]	radius, Å	SCCC[d]	CNDO[e]	Fenske–Hall[f]
	charge	κ	charge	κ	charge	κ	charge	κ	charge					
Mn	−0.38 (9)	0.955 (3)	−0.70 (9)	0.942 (4)	1.30 (6)	0.938 (3)	1.05 (7)	0.922 (3)	−0.35 (12)	−0.35	1.31	0.33	1.02	
$C_{bridging}$	0.04 (14)	1.050 (9)	0.58 (17)	1.073 (11)	−0.32 (14)	1.024 (9)	0.20 (18)	1.038 (10)	−0.09 (12)	0.14	1.10	−0.81	−0.33	−0.53
$H_{methylene}$	0.12 (7)	1.233 (33)	−0.06 (9)	1.133 (27)	0.10 (7)	1.237 (32)	−0.08 (9)	1.094 (26)		0.12[b]		−0.05	0.08	
$O_{carbonyl}$	−0.27 (5)	0.993 (2)	−0.25 (5)	1.003 (3)	−0.33 (5)	0.990 (2)	−0.32 (5)	0.998 (3)	−0.36 (7)	−0.13	0.99		−0.42	
$C_{carbonyl}$	0.16 (6)	1.049 (4)	0.14 (6)	1.053 (4)	−0.07 (6)	1.030 (4)	−0.11 (6)	1.031 (4)	−0.28 (7)	−0.05	0.98	0.16	0.26	
C_{Cp}	−0.09 (6)	1.047 (2)	−0.02 (6)	1.056 (2)	−0.18 (5)	1.039 (2)	−0.14 (6)	1.046 (2)	−0.31 (7)	−0.08	1.02		−0.26	
H_{Cp}	0.18 (5)	1.278 (19)	0.16 (5)	1.272 (18)	0.09 (5)	1.254 (17)	0.10 (5)	1.211 (16)		0.18[b]		−0.23	0.13	
CH_2 group	0.28		0.49		−0.12		0.04			0.38				
	4.81		2.78		1.52		0.38							

	Mn valence shell $3d^54s^2$		Mn valence shell $3d^7$			Mn valence shell $3d^54s^2$		Mn valence shell $3d^7$	
	IA	IIA	IB	IIB		IA	IIA	IB	IIB
N_{var}	24	137	24	137					
$R(F)$	0.0402	0.0393	0.0400	0.0391	$R_w(F)$	0.0396	0.0353	0.0394	0.0352
$R(F^2)$	0.0585	0.0544	0.0576	0.0537	$R_w(F^2)$	0.0798	0.0711	0.0795	0.0711

[a] See text. [b] Assumed, as in refinement IA. [c] Sum of charges without constraints. [d] This work. [e] Reference 27. [f] Reference 7.

(22) F. Takusagawa, A. Fumagalli, T. F. Koetzle, and W. A. Herrmann, *Inorg. Chem.*, **20**, 3060 (1981).
(23) L. J. Guggenberger and R. R. Schrock, *J. Am. Chem. Soc.*, **97**, 6578, (1975), and references therein.
(24) (a) P. Coppens, T. N. Guru Row, P. Leung, E. D. Stevens, P. J. Becker, and Y. W. Yang, *Acta Crystallogr., Sect. A*, **A35**, 63 (1979); (b) P. Coppens, *Isr. J. Chem.*, **16**, 159 (1977).
(25) W. C. Hamilton in "Statistical Methods in the Physical Sciences", Ronald Press, New York, 1964, Section 4-5.

3d shell was also considered. All the scattering factors were taken from ref 15, except Mn 4s.[26]

Table V summarizes the essential results, obtained with the two assumed configurations of Mn (columns A and B). For each configuration two types of refinement were performed: (I) only the charge parameters κ and q refined, the positional and thermal parameters being fixed at their high-angle refinement values (number of variables N_{var} = 24); (II) all parameters refined, except those of the hydrogen atoms, fixed at their full-angle refinement values (N_{var} = 137).

Owing to its strong correlation with the contraction coefficient κ of Mn (correlation coefficient −0.92), the scale factor was fixed at the value given by the conventional refinement on all X-ray data (2.5013). However, so that which way the handling of the scale factor could influence the final results could be ascertained, a conventional refinement on scale, positional, and thermal parameters was performed with the Mn $3d^7$ configuration. The largest variation was on the scale factor with a final value of 2.4257 (42). The IB and IIB refinements were then repeated with this new scale factor, and the largest change was obtained for the Mn κ parameter (1.094 (3) and 1.003 (3) for IB and IIB, respectively), but all other charge parameter changes were within their standard deviation. ΔQ is the change that would occur in the total number of electrons in the asymmetric unit if no charge constraint was applied.

Table V contains also the results of a charge integration in real space. The integration volumes are spheres centered on the atomic nuclei, the radii being defined by the condition of zero charge for the free-atom model.[9] The advantage of this procedure is that the volumes of integration are well-defined; the disadvantage is that they do not completely fill the space and that they are intersecting. This gives negative charges on all atoms as a consequence of counting the valence electrons twice in two intersecting spheres. In the case of C–O bonds, on which there is a large electron accumulation, the valence electrons belonging to two intersecting spheres are attributed at the same time to each atom; in the case of the cyclopentadienyl C–C bonds the valence electron density is lower but the sphere of integration includes part of the C–H bond electrons, so that we may roughly admit the same bias for all C and O atoms. The Mn–ligand overlap is much smaller, and the charge of Mn is thus probably genuinely negative. An approximate normalization may be carried out by adding a common quantity to all C and O charges in order to insure electron neutrality.

The κ-refinement method gives a negative Mn charge when the configuration is a combination of 3d and 4s but a positive value with the $3d^7$ configuration. This is simply due to the larger volume of the Mn $3d^5\,4s^2$ atom owing to the diffuseness of the fourth shell. Indeed the 4s scattering factor falls down so rapidly that it is zero for $(\sin\theta)/\lambda = 0.19$ Å^{-1}. Since the exact proportion of 3d and 4s (or 4p) electrons is practically impossible to determine experimentally, this shows the difficulty of the metal charge determination.

Obviously, the least-squares esd's of Table V do not provide a good indication of the actual uncertainty, which is better shown by the spread of the results from the different refinement models. The same holds to some extent for the other refined parameters.

The methylene carbon charge varied in the different types of refinement from +0.58 e to −0.32 e. This charge depends not only on the assumed configuration of the metal but also on the position of the hydrogen atoms. The total charge of the methylene group is much less sensitive to its exact geometry.

(26) D. T. Cromer, unpublished data, 1977.

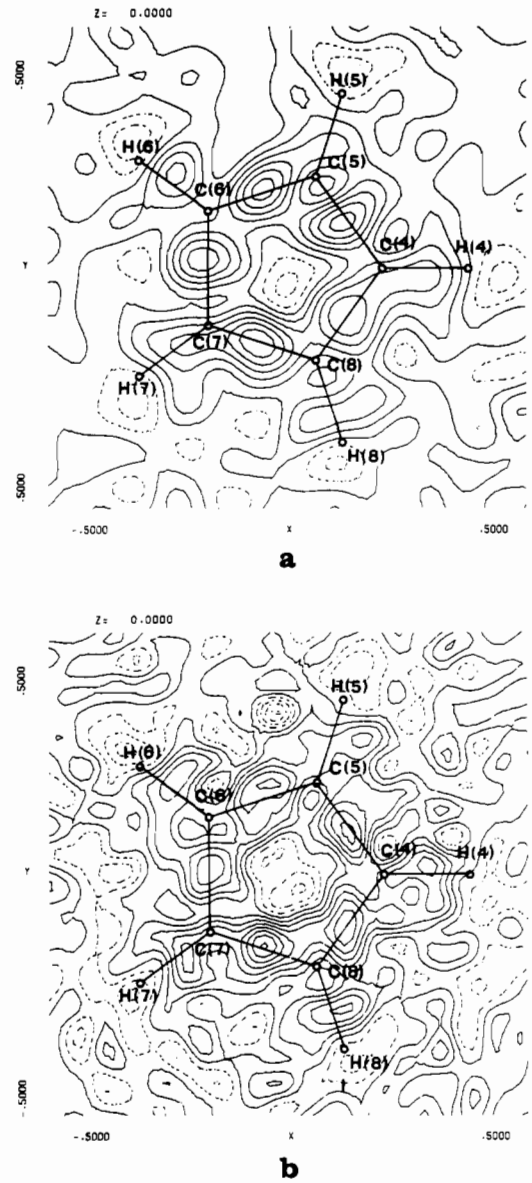

Figure 3. Observed deformation electron density in the cyclopentadienyl ring: (a) max[$(\sin\theta/\lambda] < 0.70$ Å^{-1}; (b) all reflections with $I > 3\sigma(I)$ enclosed, max[$(\sin\theta)/\lambda] < 1.06$ Å^{-1}. The contour interval is 0.1 e Å^{-3}; negative contours are shown by broken lines.

The charges of the cyclopentadienyl ring and of the carbonyl groups are more stable. In the cyclopentadienyl group the carbon atoms are always slightly negative and the hydrogens positive. In the carbonyls the oxygen atoms are always negative and the carbon atom charge is close to zero. All this is in agreement with the real-space integration and with the theoretical calculations reported in the last column of Table V.

The R factors of refinements of type II are significantly lower than those of type I. This simply means that bias of positional and thermal parameters can account for a large part of the bonding-electron rearrangements and thus compete with the charges and expansion coefficients for the description of charge distribution. A good illustration of such competition is provided by the methylene group: when the hydrogen atoms are displaced toward the carbon, they become more negative while their κ coefficient decreases, because a larger part of the bonding electrons can now be attributed to a somewhat more expanded hydrogen atom, at the expense of carbon, which becomes more positive. This example shows that the resulting charges will depend on the number and direction of bonds to which each atom participates, so that not only the refined

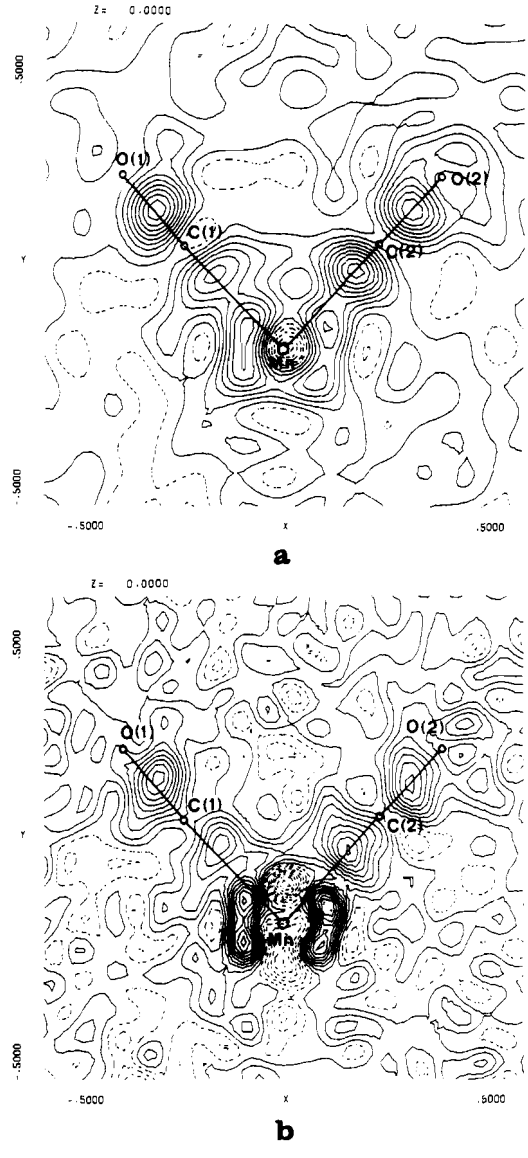

Figure 4. Observed deformation electron density in the plane of C(1)–O(1) and C(2)–O(2) carbonyl groups: (a and b) maps and contours as in Figure 3.

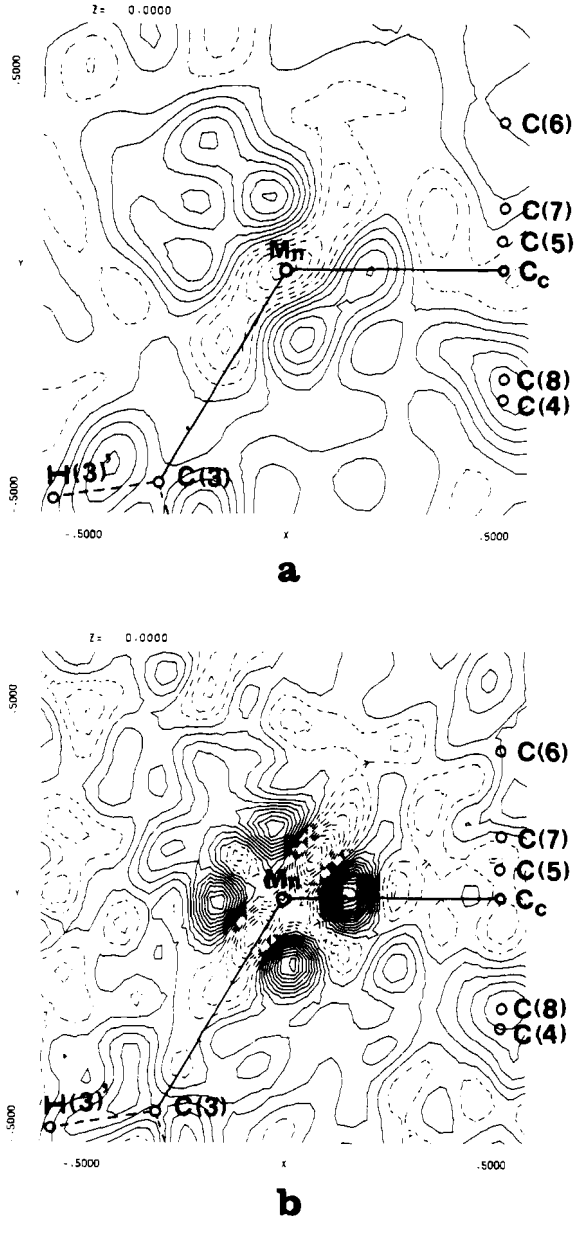

Figure 5. Observed deformation electron density in the plane defined by C(3), Mn, and C_c (C_c = centroid of the cyclopentadienyl ring): (a and b) maps and contours as in Figure 3.

positional and thermal parameters but also the atomic charges are affected by systematic bias. Model I, which is less flexible but presents less ambiguity, thus seems preferable.

In a general way, the best agreement between direct-space and reciprocal-space charge determinations is given for refinement IA, which is therefore the most credible. This, and the direct-space integration, gives a slightly negative charge for Mn and a methylene carbon charge not significantly different from zero. This is in contrast with theoretical calculations, which have all predicted a large negative charge on this atom,[7,8,27] as may be seen in Table V. For the reasons given above, and also because of the special position of the methylene group on the binary axis, this charge is difficult to determine experimentally. It is however unlikely to be so largely negative.

Electron-Density Distribution

The X–X deformation density $\Delta\rho(x,y,z)$ at a point x, y, z was computed as $\Delta\rho(x,y,z) = \rho_{crystal}(x,y,z) - \sum\rho_{free\ atoms} = \rho_{obsd}(x,y,z)/K - \rho_{calcd}(x,y,z)$, where ρ_{obsd} is the Fourier transform of the unscaled observed structure factors, corrected for anomalous dispersion effects, and ρ_{calcd} is the density calculated in the spherical atom approximation (ground state) with use of atomic parameters derived from the high-angle refinement. Two series of density maps are shown in Figures 3–8, computed at two resolutions: (a) to a maximum ($\sin\theta/\lambda$ value of 0.70 Å^{-1}; (b) to the largest ($\sin\theta$)/λ of the measurements, 1.06 Å^{-1}, with the additional condition $I > 3\sigma(I)$, to avoid an excessive background. Unless explicitly stated otherwise the deformation densities discussed hereafter are those of the lower resolution.

The scale factor K is often determined by a least-squares refinement in which positional and thermal parameters are fixed at their high-angle values; however, we have found during the high-angle refinement that K is highly correlated with the Mn thermal parameters (correlation factors $\simeq$0.85). The scale factor was therefore fixed at the value of the full refinement.

The esd due to random errors, at some distance from the atomic centers and from the binary axis, is 0.061 e Å^{-3} on the low-resolution maps and 0.176 e Å^{-3} on the high-resolution maps, including the reflections with $I < 3\sigma(I)$ in the esd calculation, while this esd falls to 0.078 not including these reflections.

(27) G. Granozzi, E. Tondello, M. Casarin, and D. Ajò, *Inorg. Chim. Acta*, **48**, 73 (1981).

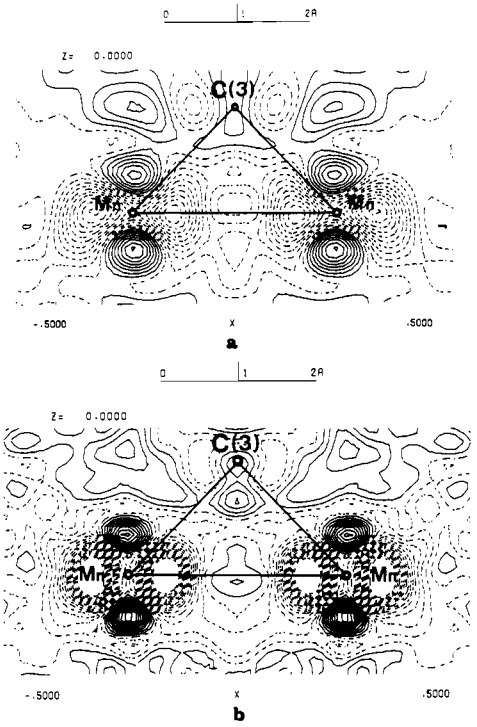

Figure 6. Observed deformation electron density in the dimetallacyclopropane ring Mn, C(3), Mn′: (a and b) maps and contours as in Figure 3.

Table VI. Mulliken Electron Populations from SCCC MO Calculations for Title Compound (A), $(\mu\text{-}CO)[CpMn(CO)_2]_2$ (B), and $CpMn(CO)_3$ (C)

	A	B	C
	Orbital Populations for Mn		
$3d_{z^2}$	1.81	1.76	1.72
$3d_{x^2-y^2}$	1.64	1.63	1.49
$3d_{xy}$	1.22	1.33	1.49
$3d_{yz}$	0.89	0.78	0.87
$3d_{xz}$	0.84	0.93	0.87
4s	0.19	0.17	0.10
$4p_x$	0.07	0.08	0.08
$4p_y$	0.02	0.03	0.08
$4p_z$	0.01−	0.00	0.01
	Metal and Ligand Charges		
Mn	0.33+	0.28+	0.28+
C(1)O(1)	0.14+	0.03+	0.04+
C(2)O(2)	0.18+	0.08+	0.04+
C(3)O(3)		0.05−	0.04+
$C(3)H_2$	0.91−		
C_5H_5	0.23−	0.37−	0.40−
	Overlap Populations		
Mn-Mn	0.06	0.03	
Mn-C(3)	0.28		
Mn-C(1)O(1)	0.45	0.46	0.46
Mn-C(2)O(2)	0.43	0.43	0.46
Mn-C(3)O(3)		0.29	0.46
Mn-C_5H_5	0.53	0.49	

The deformation density in the two carbonyl regions resembles other CO deformation maps;[9,21] prominent peaks are seen in the C–O bond regions (0.84 and 0.73 e Å^{-3}) as well as in the carbon lone-pair region (0.82 and 0.51 e Å^{-3}); the oxygen lone pairs are more diffuse, and this is certainly due in part to thermal motion and in part to a bias of the X–X technique that shifts the O atoms toward their lone pair, since this contributes to the high-order reflections.[28] Indeed, at least

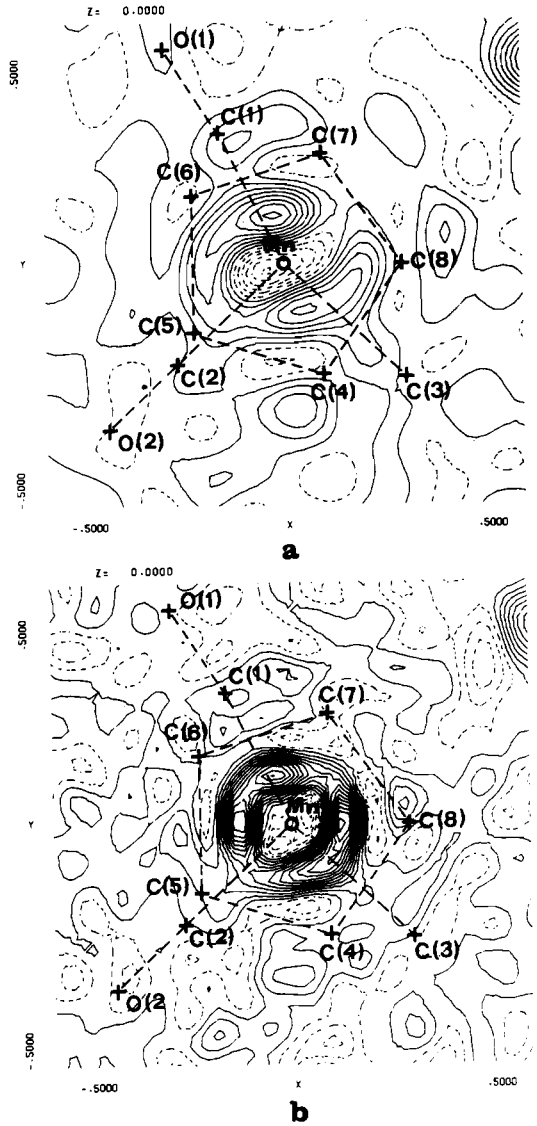

Figure 7. Observed deformation electron density in a section through the Mn atom and parallel to the cyclopentadienyl ring: (a and b) maps and contours as in Figure 3.

for O(2), the peak is higher at high resolution (Figure 4b).

By contrast the deformation density between the two Mn atoms, in the central region of the metal–metal bond, is near zero in the low-resolution maps and only slightly positive (0.10 e Å^{-3}) but not significant at the highest resolution. The same observation has been made in most of the metal–metal-bonded compounds studied so far by X–X or X–N methods.[9,21,29,30] Only in the shortest quadruple metal–metal bonds was a significant overlap charge observed.[31,32]

Bonds between transition metals of the left side of the periodic table may exhibit a double maximum on the deformation density. This was observed in Ti_2O_3.[33] The reason is that the most favorable occupancy of the d_{z^2} orbital (z being along the metal–metal bond) in the "prepared" atom prior to the formation of a σ bond is one electron, that is, more than the occupancy in the spherically averaged atom. The situation

(28) J. W. Bats, P. Coppens, and T. F. Koetzle, *Acta Crystallogr., Sect. B*, **B33**, 37 (1977).
(29) M. Benard, P. Coppens, M. L. De Lucia, and E. D. Stevens, *Inorg. Chem.*, **19**, 1924 (1980).
(30) W. Geibel, G. Wilke, R. Goddard, C. Krueger, and R. Mynott, *J. Organomet. Chem.*, **160**, 139 (1978).
(31) K. Hino, Y. Saito, and M. Bénard, *Acta Crystallogr., Sect. B*, **B37**, 2164 (1981).
(32) A. Mitschler, B. Rees, R. Wiest, M. Benard, to be submitted for publication.
(33) G. Vincent, K. Yvon, A. Gruttner, and J. Ashkenazi, *Acta Crystallogr., Sect. A*, **A36**, 803 (1980).

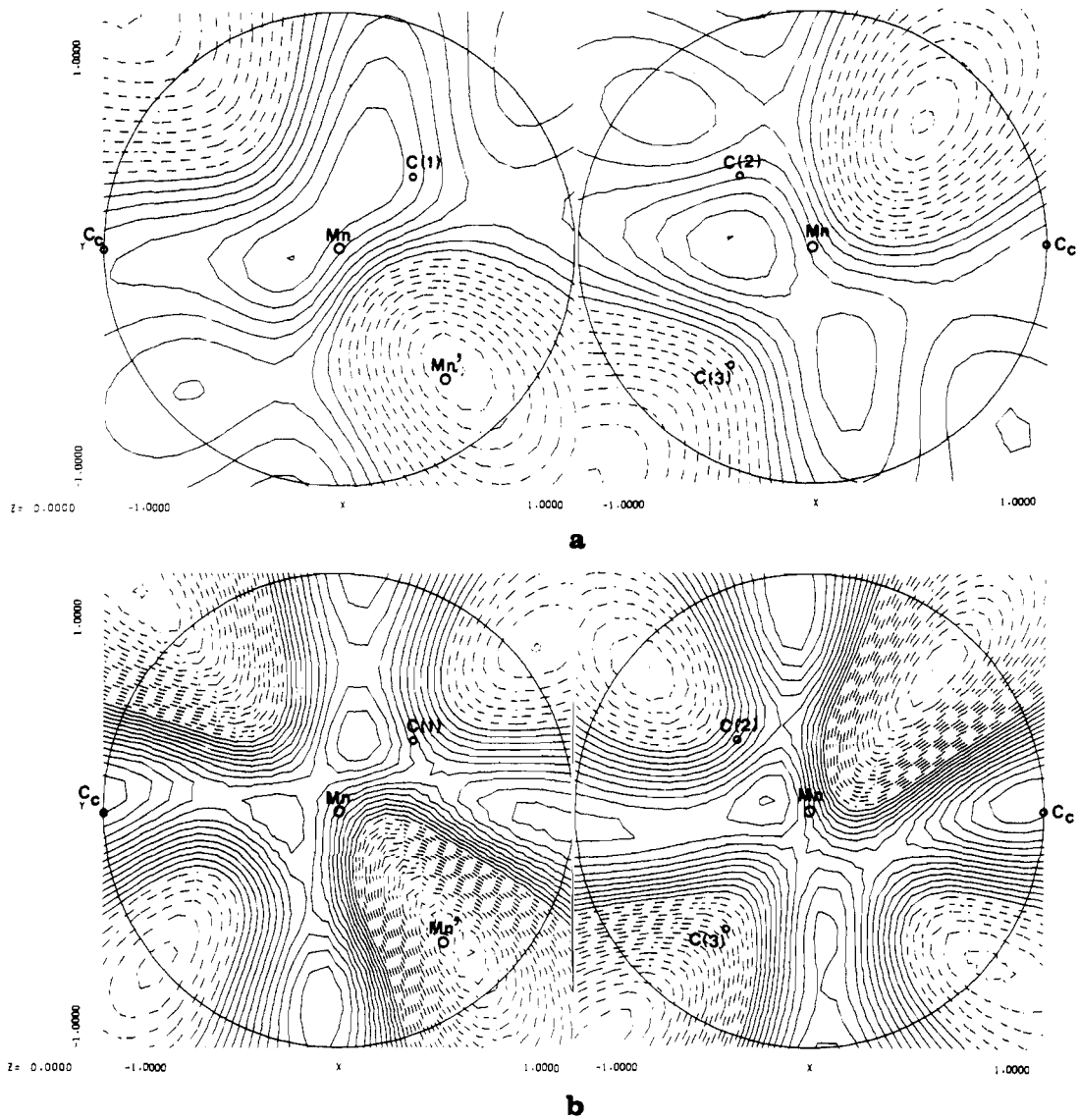

Figure 8. Observed deformation electron density in a section defined by a sphere of radius 0.60 Å centered on Mn: (a and b) maps and contours as in Figure 3.

is reversed for metals with more than five electrons in the 3d shell. The double minimum observed here in the Mn–Mn bond is consistent with this description.

A significant charge gradient is found along the $Mn–CH_2$ line with a zone of charge accumulation close to the methylene carbon atom (0.15 e $Å^{-3}$) that increases to 0.31 e $Å^{-3}$ in the map at high resolution, indicating a valence-shell contribution to the high-order reflections. The σ lone pair of methylene thus gives a rather sharp peak in the deformation density. This probably leads to a small bias in the carbon position as determined from high-order X-ray data, and one would expect a higher peak in a X–N deformation density.

Around the Mn nucleus there are several regions of high electron density with peaks at a distance of approximately 0.60 Å, the distance at which the largest effect of unequal occupation of the 3d electrons is expected. However caution is needed in the interpretation, because this is also the region where systematic errors would show up. As expected, at high resolution, the metal asphericity features become considerably sharper. The density around the metal nucleus is centrosymmetric, which seems to indicate that there is little mixing of the 4p with the 3d orbitals (combination of odd and even functions would result in noncentrosymmetric features).

Looking at the deformation density in a section of a sphere of radius 0.60 Å centered on the metal nucleus (Figure 8), one observes that the density is located principally along the $Mn–C_c$ axis and in a plane passing through the metal atom and nearly perpendicular (80°) to $Mn–C_c$. Particularly noteworthy is the maximum at 0.71 Å from Mn in the direction of the Cp ring that increases 1.31 e $Å^{-3}$ in the high-resolution map. Similar features were found in $[CpFe(CO)_2]_2$, with an approximate cylindrical symmetry around the $Fe–C_c$ axis. This cylindrical symmetry is here somewhat distorted, probably because of the lower symmetry and the distortion of the $Mn(CO)_2CH_2$ fragment.

For a better understanding of the bonding we performed a simple semiempirical molecular orbital calculation of the SCCCMO type.[34] The geometry of the molecule was

(34) D. A. Brown and R. M. Rawlinson, *J. Chem. Soc. A*, 1534 (1969). The present calculation used the following basis set (and corresponding VOIP's in eV): for the carbonyls 1π (−16.9), 5σ (−14.0), and 2π (−6.0); for cyclopentadienyl the π orbitals a (−13.927), e_1 (−10.976), and e_2 (−5.476); for methylene C(2s) (−19.47), C(2p) (−10.66), and H(1s) (−13.64); for Mn the 3d, 4s, and 4p orbitals (charge and configuration dependent VOIP's as tabulated by H. Basch, A. Viste, and H. B. Gray, *Theor. Chim. Acta*, 3, 458 (1965)). The Slater exponents of the atomic orbitals were as follows: H(1s), 1.30; C(2s), 1.61; C(2p), 1.57; O(2s), 2.25; O(2p), 2.23; Mn(3d), 5.15 and 1.90 (with contraction coefficients 0.532 and 0.649); Mn(4s), 1.45; Mn(4p), 0.90. Off-diagonal terms of the H matrix were after L. C. Cusachs, *J. Chem. Phys.*, 43, S157 (1965).

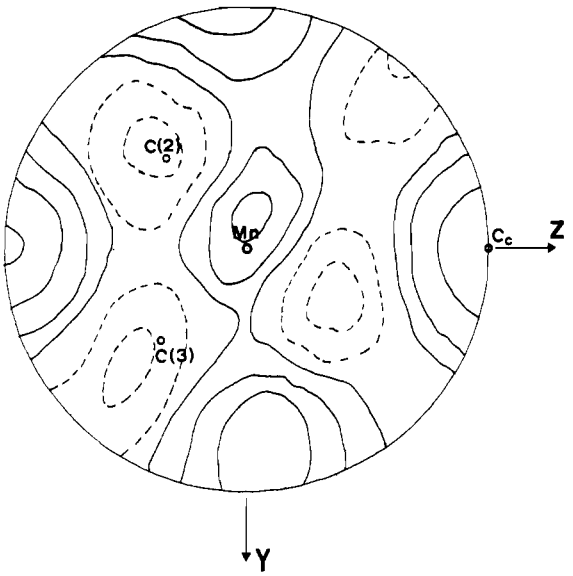

Figure 9. Theoretical asphericity of d orbitals around the Mn atom in units of $[R(r)]^2/4\pi$. The axes chosen for the MO calculation are also shown.

idealized, with use of the program CDNT written by J. M. Howell at Cornell University, with Mn–C–O angles of 180°.

For a clear comparison with $CpMn(CO)_3$ the z axis was taken perpendicular to the cyclopentadienyl ring and the y axis along C_c–C(8). Table VI reports some results of the Mulliken electron population analysis. It is interesting to note that the lack in cylindrical symmetry around z is correctly predicted by the SCCC calculation, as the occupancy of $d_{x^2-y^2}$ is larger than that of d_{xy} (1.64 against 1.22). This asymmetry is due not only to the distortion of the $Mn(CO)_2CH_2$ fragment but also to the substitution of a CO group by a methylene group: in column B of Table VI we report the results of a SCCC computation on the hypothetical compound $(\mu\text{-}CO)[CpMn(CO)_2]_2$, where the methylene has been substituted by a carbonyl. The $d_{x^2-y^2}$ and d_{xy} occupancies become closer. In the symmetrical molecule $CpMn(CO)_3$ the $d_{x^2-y^2}$ and d_{xy} orbital charges are both equal to 1.49 and thus we expect a perfect cylindrical symmetry in the xy plane.

When it is compared to the two other compounds, there is in the methylene-bridged complex a negative charge transfer to the methylene group. This charge is taken from the whole $CpMn(CO)_2$ moiety but predominantly from the ligands rather than from the metal.

Finally, we have calculated a theoretical asphericity of the 3d electron density around the Mn nucleus[21]

$$\Delta\rho(r) = \sum_{\mu}\sum_{\nu} P_{\mu\nu}(\phi_\mu(r))(\phi_\nu(r)) - \rho_0(r)$$

where the double sum is over the five 3d orbitals, P is the first-order density matrix, and $\rho_0(r)$ is the spherical average of the first term. With the d orbitals $\rho_\mu(r)$ written as $(R(r))(y_\mu(\theta,\phi))$, the function

$$4\pi(\Delta\rho(r))/R^2(r) = 4\pi\sum_{\mu}\sum_{\nu} P_{\mu\nu}(y_\mu(\theta,\phi))(y_\nu(\theta,\phi)) - \sum_{\mu} P_{\mu\mu}$$

is plotted in stereographic projection in Figure 9 (only one hemisphere is shown; the second is obtained through inversion, due to the parity of d orbitals). There is a quite good agreement with the experimental high-resolution maps of Figure 8b. Even the tilting angle of the high-density plane (vertical in the figures) relative to the Mn–C_c direction is reproduced. The improvement of the experimental maps at higher resolution is again striking. We may conclude that the asphericity of density around Mn is essentially due to unequal occupancy of the 3d orbitals, which is correctly predicted by the SCCC MO calculation. A former study on $[CpFe(CO)_2]_2$[21] had reached the same conclusion.

Acknowledgment. We are grateful to Strasbourg University (Strasbourg, France) for providing computing facilities. We thank Dr. Roland Wiest and Andrê Mitschler for useful discussions. D.A.C. is indebted to NATO for a senior fellowship that allowed him to spend 4 months at Strasbourg University. We are also grateful to the Italian computing centers CINECA (Casalecchio di Reno) and CNUCE (Pisa).

Registry No. $(\mu\text{-}CH_2)[CpMn(CO)_2]_2$, 57603-41-5.

Supplementary Material Available: Listings of calculated and observed structure factors, anisotropic thermal parameters U_{ij}, and least-squares molecular planes and associated angles (41 pages). Ordering information is given on any current masthead page.